


# Radial Support Force: A Key Player in Vena Cava Neointimal Hyperplasia

Maofeng Gong<sup>1</sup>, Rui Jiang<sup>1</sup>, Kang Guo<sup>2</sup>, Xu He<sup>1</sup>, Jianping Gu<sup>1</sup> 

<sup>1</sup>Department of Interventional and Vascular Radiology, Nanjing First Hospital, Nanjing Medical University, Nanjing, Jiangsu, 210006, People's Republic of China; <sup>2</sup>Imaging Department of Yixing Traditional Chinese Medicine Hospital, Yixing, Jiangsu, 214200, People's Republic of China

Correspondence: Jianping Gu, Email gujianpingnj@163.com

**Background:** Neointimal hyperplasia (NIH) is a risk factor for inferior vena cava filter (IVCF) retrieval failures and damage to the inferior vena cava (IVC) wall post-retrieval. Unfortunately, the mechanical properties of IVCFs have not been evaluated and are not readily available from the manufacturer. This study aimed to investigate the correlations between radial support force (RSF) and NIH, and the release of tumor necrosis factor-alpha (TNF- $\alpha$ ) during this process.

**Methods:** RSFs exerted by IVCF struts at various IVC diameters were analyzed with five replicates in vitro. In vivo, Bama swine were randomly fitted with IVCFs of 32 mm or 20 mm diameter. After a dwelling time of three weeks, the thickness of NIH and TNF- $\alpha$  content in the areas adjacent to IVCF struts were determined on hematoxylin and eosin. Correlations were assessed using Student's *t*-test, chi-square test, and regression analyses.

**Results:** A mismatch between IVC and IVCF diameter generated an oversizing ratio (OR), with a mean OR of  $113.06 \pm 48.91\%$  (range, 61.73–166.52%). RSFs of  $4.56 \pm 0.97$  N (range, 3.54–5.61 N) showed a linear dose-response relationship with ORs ( $R^2 = 0.718$ ,  $p < 0.001$ ). NIH thickness increased with the enlarged RSFs, and regression analyses demonstrated a U-shaped dose-response relationship ( $R^2 = 0.630$ ,  $p < 0.001$ ). A larger TNF- $\alpha$  content at minimal caval diameter was observed with increased RSFs, indicating a more severe presence of TNF- $\alpha$  following the increased RSF ( $R^2 = 0.777$ ,  $p < 0.001$ ).

**Conclusion:** Differences in RSFs are consistent with ORs; RSFs increased with the larger ORs of IVCF and IVC diameter. Increased RSFs correlate with greater NIH thickness. Evaluation of IVCF yielded a significantly higher RSF at a smaller caval diameter, with higher levels of TNF- $\alpha$  during expansion, supporting a close association with greater NIH.

**Keywords:** neointimal hyperplasia, porcine model, radial support force, oversizing ratio, proliferation

## Introduction

In recent decades, cardiovascular disease (CVD) has emerged as the leading threat to human health worldwide, surpassing cancer due to the aging global population.<sup>1</sup> By 2030, it is expected that 23.3 million people worldwide will die from CVD.<sup>1–3</sup> Acute pulmonary embolism (PE) contributes to a global burden of CVD in terms of morbidity, mortality, and financial impact on healthcare systems.<sup>3,4</sup> Inferior vena cava filter (IVCF) has been effectively used to prevent fatal PE in patients who underwent deep vein thrombosis (DVT).<sup>4</sup> However, after placement, IVCF inevitably damages the inferior vena cava (IVC) wall, triggering a series of pathological processes,<sup>1,3</sup> including clots formation and acute inflammatory response, which are interrelated and responsible for the excessive deposition of extracellular matrix and proliferation of smooth muscle cells (SMCs), which ultimately cause neointimal hyperplasia (NIH).<sup>5</sup>

In clinical practice, retrieving IVCFs as early<sup>4</sup> and completely as possible once PE protection is not needed is strongly recommended, to leave no remnants in IVC and reduce potential IVCF-related complications.<sup>6</sup> Nonetheless, the challenge of filter retrieval persists and, in some cases, proves impracticable. The overgrowth of caval NIH has been linked to failures in IVCF retrieval and detriment to the IVC wall post-retrieval.<sup>6–8</sup> IVCF removal may pose risks to the IVC, whereas prolonged retention increases the likelihood of caval occlusion. Under varying physiological conditions, physiological forces such as cyclic stretch, blood pressure, and shear stress, are believed to play crucial roles in

regulating neointimal remodeling, promoting the regeneration of injured tissues, and the phenotypic transformation of SMCs.<sup>5,9</sup> However, the impact of radial support force (RSF), a non-physiological mechanical force, derived from the struts of IVCFs, has not been well elucidated. Consequently, a significant gap remains in understanding how RSF contributes to the NIH of IVC wall.

We hypothesized that an elevated RSF may accelerate the development of NIH. Hence, we wonder whether using IVCFs with reduced RSFs could serve as a promising strategy to inhibit NIH. The pathophysiological roles of tumor necrosis factor- $\alpha$  (TNF- $\alpha$ ) in caval NIH remain unclear. Thus, the purpose of this experimental study is to explore the correlations between the RSF, NIH, and the release of TNF- $\alpha$ . This study may offer a theoretical foundation for the optimization and innovation of IVCF designs, potentially demonstrating significant NIH inhibition, reducing adhesion between the vascular wall and filter, and minimizing vascular injury during retrieval. Therefore, a better understanding is essential for designing therapeutic strategies.

## Methods and Methods

### Animals, IVCFs Used, and Anesthesia

This study followed the Guideline for Care and Use of Laboratory Animals, and the protocol was approved by the Animal Ethics Committee of Nanjing First Hospital (No. DWSY-23153536). All animals used were sourced from the Laboratory Animal Center of our Hospital. Eight Bama miniature swine (four males, four females; 45–55 weeks; 25–35 kg) were enrolled. The swine were randomly assigned to receive either 32 mm or 20 mm diameter retrievable filters (Illicium, Visee Medical Instruments Co. Ltd, Shandong, China). Sedation of the swine was achieved through intramuscular injection of ketamine hydrochloride (15 mg/kg) in combination with atropine sulfate (0.04 mg/kg). Anesthesia was carried out using an anesthesia machine (Rui Wode Life Science and Technology Co. Ltd, Shenzhen, China), delivering 5% isoflurane (100 mL/bottle, Rui Wode Life Science and Technology Co. Ltd, Shenzhen, China) through a face mask. General anesthesia was maintained using a continuous administration of isoflurane (1.5–3%) mixed with oxygen delivered at 0.8 L/min.<sup>5</sup> The schematic overview of this study design is shown in Figure 1.

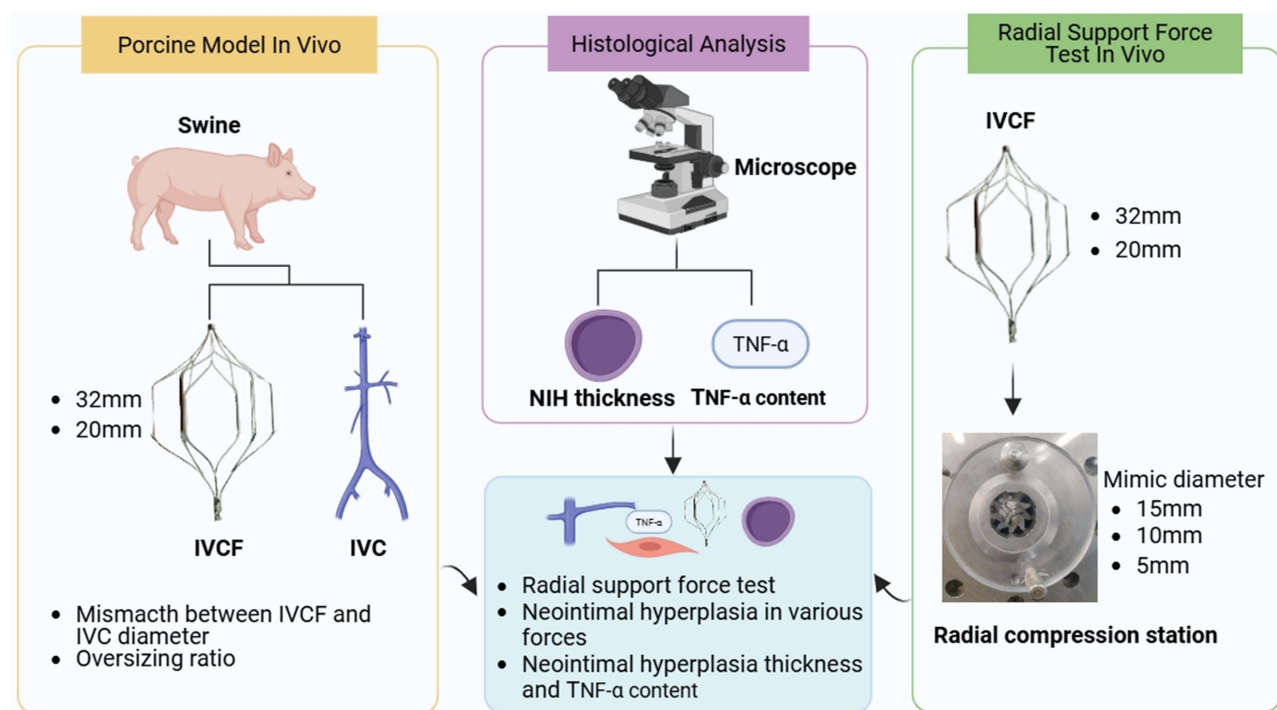


**Figure 1** Study overview. The porcine model, radial support force test in vitro, and histological analysis.

**Abbreviations:** IVC, inferior vena cava; IVCF, inferior vena cava filter; TNF- $\alpha$ , tumor necrosis factor- $\alpha$ ; NIH, Neointimal hyperplasia.

## In vitro Radial Force Tests

RSF was evaluated in vitro using a Radial Compression Station (Blockwise Engineering LLC, Tempe, AZ). IVCFs with diameters of 32 mm and 20 mm were tested in simulated IVC models with diameters of 5 mm, 10 mm, and 15 mm at  $37 \pm 2^\circ\text{C}$ . RSFs generated by the IVCF were measured in real time. Each measurement was performed five times, and the replicate data were averaged.

## In vivo Experimental Design and Procedures

As previously reported,<sup>5</sup> interventional procedures were performed following strict aseptic conditions. The images were taken in both anterior-posterior and lateral views using a non-ionic contrast agent (Iodixanol, 370 mgI/mL, Bayer Schering Pharma, Germany) injected at a rate of 5.0 mL/s with a total volume of 15 mL to evaluate IVC diameter and renal vein position. All swine were administered a heparin bolus (50 units/kg) prior to IVCF deployment. Each IVCF was introduced through the filter-release sheath via the right or left femoral vein. Under fluoroscopy guidance to confirm the renal veins, the filters were deployed approximately 2–5 mm below the infrarenal IVCs. If the filter tilted  $> 15^\circ$ , it was repositioned and redeployed. Each swine received an antibiotic (10 mg/kg, cefradine) intramuscularly for three consecutive days for antibiotic prophylaxis. As a prophylactic measure against thrombosis, low molecular weight heparin (Enoxaparin, 40 mg; Sanofi, Madrid, Spain) was administered once daily. At the 3rd week, venography was performed through the same femoral vein to evaluate the positioning of the IVCF and detect any possible complications.

## Measurement of IVC Diameter and OR

Three-dimensional (3D) digital subtraction angiography (DSA) imaging was employed to measure the diameter of the IVC below the renal vein in swine.<sup>5</sup> This technique helped identify the optimal viewing angle to accurately determine both the minimum and maximum IVC diameters. After IVCF placement, the mean diameter of the IVCF was measured, and OR could be calculated using the following equations.<sup>5</sup>

$$\text{OR} = \left( \frac{\text{IVCF diameter}}{\text{IVC diameter}} - 1 \right) \times 100\% \quad (1)$$

## Hemodynamics Evaluation Pre- and Post-IVCF Placement

As reported in our previous study concerning artery disease,<sup>10</sup> the preprocedural and postprocedural DSA data were promptly transferred to a dedicated workstation (syngo X Workplace VB21; Siemens) to generate color-coded DSA (ccDSA) images (syngo iFlow; Siemens). This procedure translated the time delay between the injection of contrast material and the peak opacification on a pixel-by-pixel basis into specific colors, ranging from red (early peak density) to blue (late peak density). The color-coded maps generated were used to create curves illustrating the changes in contrast intensity over time for each chosen region within the image. Regions of interest (ROIs) were selected from the initial and final ccDSA images to assess the hemodynamic alterations induced by the placed IVCF. First, a small ROI was established as a reference baseline for the patient's blood flow. Next, additional small ROIs were placed where the IVCF contacts the IVC wall to evaluate the hemodynamic impact of the IVCF. Time–intensity curves were generated for each ROI, from which the time-to-peak (TTP) parameter was derived.

## Tissue Sampling and Histological Analysis

All swine were euthanized three weeks after IVCF placement via intravenous administration of 10% potassium chloride (0.5mL/kg) coupled with 2% lidocaine (5mg/kg). During necropsy, the IVC was carefully harvested to obtain tissue for gross evaluation of NIH, evaluation IVCF strut adhesion to the intima, and characterization of the neointimal response. The excised IVC specimens were promptly fixed in  $4^\circ\text{C}$  formalin overnight, then rinsing with distilled water. Subsequently, the tissues underwent graded alcohol dehydration and paraffin embedding. Pathology analysis was conducted in a blinded manner; a professor, unaware of the details of animal randomization and IVCF diameter, reviewed all specimens and performed the analyses.

Microscopic analysis was conducted to assess the intima and vascular wall responses in regions adjacent to the IVCF struts. Cross-sectional slices of venous tissue, 3 to 5  $\mu\text{m}$ , were routinely stained with hematoxylin and eosin (H&E) for microscopic analysis. The stained issue was analyzed at  $20\times$  magnification using pathological color image analysis software (version 2.4.0; 3D Histech Ltd., Budapest, Hungary), integrated with a microscopic imaging system. NIH thickness was measured at six distinct points from the intimal layer to the IVCF strut.

TNF- $\alpha$  immunostaining was used to quantify the proportion (%) of TNF- $\alpha$  positive areas within the vessel wall. Image analysis was performed using Image J software (version 1.50; National Institutes of Health, Bethesda, MD) on randomly selected vessel fields from each section. Given the predominance of TNF- $\alpha$  in the vascular wall, the percentage of TNF- $\alpha$  stained area was calculated to assess the TNF- $\alpha$  content. For each tissue section, six fields of view were selected, and within each,  $2\text{cm} \times 3\text{cm}$  area was analysed. The mean TNF- $\alpha$  content was measured to indicate the quantity of TNF- $\alpha$  present in the tissue, calculated using the formula below. A higher percentage value corresponds to a greater TNF- $\alpha$  presence, reflecting more significant TNF- $\alpha$  alterations.

$$\text{TNF} - \alpha \text{ Content}(\%) = \frac{\text{TNF} - \alpha (\text{cm}^2)}{\text{IVC area}(\text{cm}^2)} \times 100\% \quad (2)$$

## Statistical Analysis

All statistical analyses were conducted using SPSS software (version 22.0; SPSS Inc., Chicago, IL, USA) and R software (version 4.2.3; R Foundation for Statistical Computing, Vienna, Austria). Continuous variables with normal distribution were expressed as mean  $\pm$  standard deviation (SD), and differences between groups were evaluated using Student's *t*-test. Categorical data were summarized as numbers (percentages) and compared via the Chi-square test. Lin concordance correlation coefficient (CCC) was conducted using the MedCalc software (version 22.009, Mariakerke, Belgium) to evaluate the inter-rater agreement concerning IVC diameter. It was categorized into poor ( $\text{CCC} \leq 0.40$ ), fair to good ( $0.40 < \text{CCC} \leq 0.75$ ), or excellent ( $\text{CCC} > 0.75$ ). The associations among OR, RSF, NIH, and TNF- $\alpha$  were analyzed using regression analysis. A two-tailed *p*-value  $< 0.050$  was regarded as statistically significant.

## Results

### Technical Feasibility

Technical successes of the IVCF placement model and specimen were achieved in all swine (8/8). None of the swine died or experienced procedure-related complications, including major bleeding, angulation ( $>15^\circ$ ), migration ( $>10\text{ mm}$ ), thrombosis, and penetration ( $> 3\text{mm}$ ), and infection.

### In vitro Tests of the Relationship Between RSF and OR

The analysis of the RSFs of IVCF devices and ORs demonstrated a linear dose-response relationship in vitro, with a correlation coefficient ( $R^2 = 0.718$ ,  $p < 0.001$ ). This relationship was shown in Figure 2, and can be mathematically expressed as follows:

$$\text{RSF(N)} = 8.09 \times e^{-3} \times \text{OR}(\%) + 3.31 \quad (3)$$

Where RSF denotes the radial support force (in Newtons (N)), and OR represents the oversizing ratio (in %), illustrating the correlation between the IVCF's RSF and its size relative to the IVC diameter.

### IVC Morphology, Magnification, OR, and Hemodynamics Changes

IVC venography before IVCF placement showed an oval shape with a mean maximum and minimum IVC diameter of  $15.64 \pm 0.64\text{ mm}$  (range, 14.13–16.13 mm) and  $6.16 \pm 0.59\text{ mm}$  (range, 5.65–7.20 mm) at the intended site of IVCF deployment, respectively. Following the use of IVCF, the IVC morphology changed to a circular IVC. Lin CCC of .974 between the mean maximum and minimum IVC diameter (95% CI, 0.884–0.994). The mean IVC diameter after filter placement was measured as  $12.18 \pm 0.50\text{ mm}$ , and the mean OR and RSF were  $113.06 \pm 48.91\%$  (range, 61.73–166.52%) and  $4.56 \pm 0.97\text{ N}$  (range, 3.54–5.61 N). The TTP *post*-IVCF placement in iFlow image, as depicted in Figure 3, was  $5.03 \pm 0.73\text{ s}$ , which was not significantly different from that of  $4.98 \pm 0.70\text{ s}$  *pre*-IVCF placement ( $p = 0.756$ ).



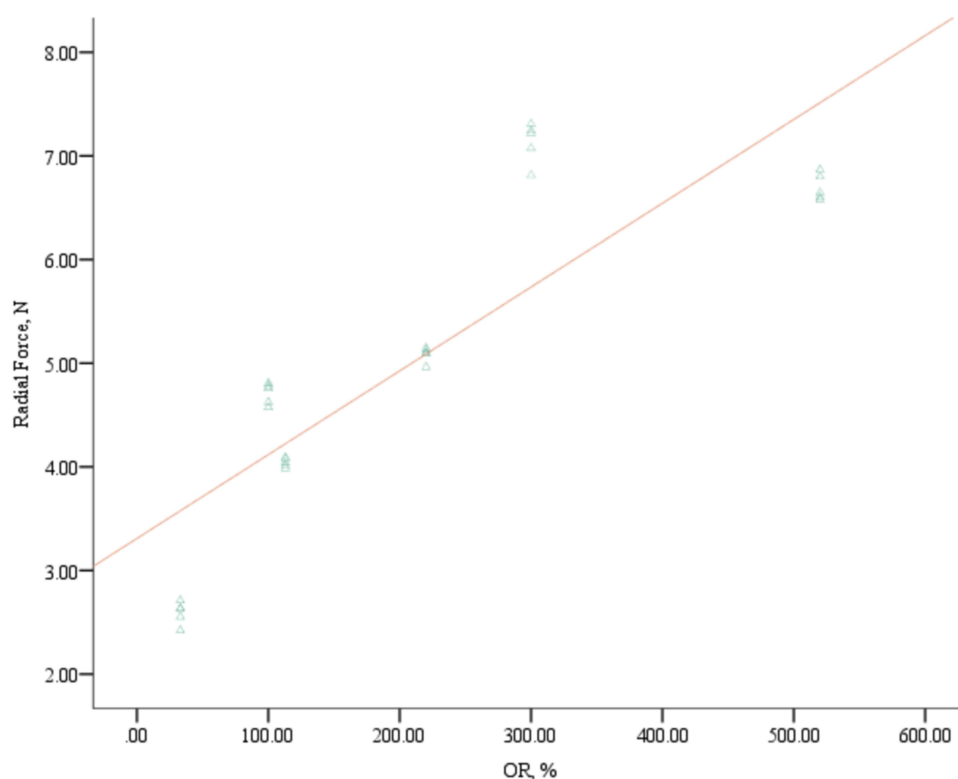


**Figure 2** RSF increase correlates linearly with OR. The relationship between the RSFs of IVCF devices can be mathematically represented as  $RSF(N) = 8.09 \times e^{-3} \times OR(\%) + 3.31$ , suggesting that RSFs consistently increased as the ORs increase ( $R^2 = 0.718$ ,  $p < 0.001$ ).

**Abbreviations:** RSF, radial support force; OR, oversizing ratio; IVC, inferior vena cava.

## In vitro Macroscopical and H&E Characterization of IVC After IVCF Placement

The macroscopic presentation of retrieved IVCFs at the 3rd week revealed a marked vascular response in the caval wall, characterized by vessel wall proliferation. NIH was macroscopically observed at the filter placement site, with more substantial thickening observed in regions directly contacting the IVCF struts (Figure 4A).

H&E staining showed subintimal thickening that had enveloped the IVCF struts; this subintimal thickening revealed hyperplasia and hypertrophy of the intimal layer, with a thin media and adventitia layer (Figure 4B), mainly resulting from the proliferation of non-striated muscle cells. The normal three-layer structure of the vessel wall was disrupted, with significant thickening of the intima and thinning of both the media and adventitia (Figure 4C). As illustrated in Figure 5, NIH thickness increased with larger filter diameters. Specifically, the IVCF with a 32 mm diameter exhibited significantly greater NIH thickness compared to the 20 mm filter ( $p < 0.05$ ), indicating more pronounced neointimal proliferation associated with increased RSF. To further evaluate the relationship between RSF and NIH thickness, regression analysis was conducted ( $R^2 = 0.630$ ,  $p < 0.001$ ), which can be expressed mathematically as follows:

$$NIH \text{ thickness}(\mu) = 2.76 \times e^3 - 1.22 \times e^3 \times RSF(N) + 1.53 \times e^2 \times RSF^2(N) \quad (4)$$

## Inflammation Analyses of TNF- $\alpha$

The presentations of TNF- $\alpha$  are shown in Figure 6. The entire trajectory of the IVCF strut was covered by TNF- $\alpha$  deposition in various RSFs. Image analysis provided the semiquantitative results, revealing varying levels of TNF- $\alpha$  expression corresponding to IVCFs of different diameters. The content of TNF- $\alpha$  increased with the increased RSFs. These implied a more severe TNF- $\alpha$  present following the increased RSF ( $R^2 = 0.777$ ,  $p < 0.001$ ). As well, synthetic SMCs was observed in the proliferation of IVC wall. The relationship can be mathematically represented.

$$TNF - \alpha \text{ Content}\% = 70.94 - 34.33 \times RSF + 4.46 \times RSF \times RSF \quad (5)$$

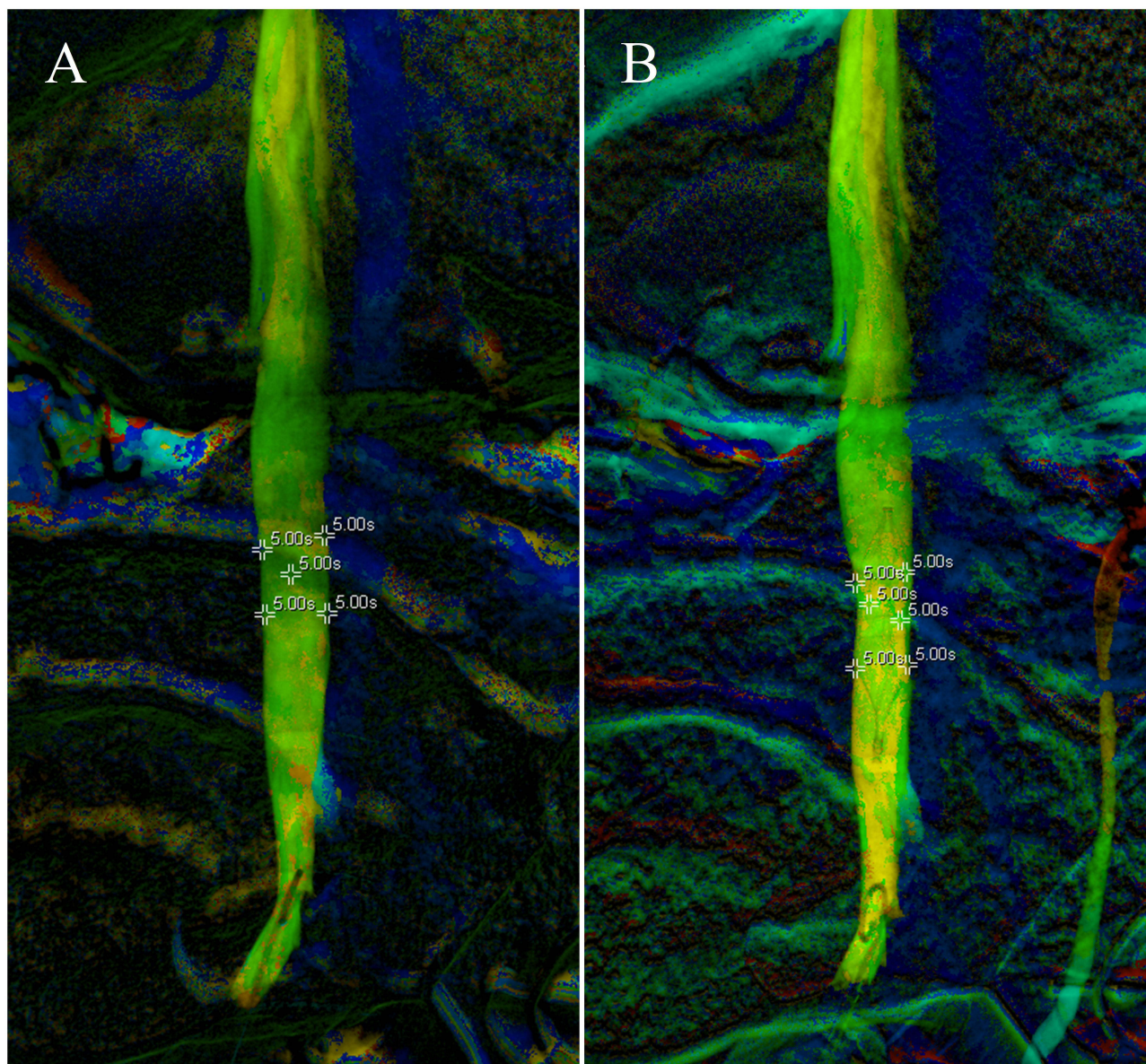


**Figure 3** Hemodynamics analysis using syngo iFlow before and after IVCF placement. **(A)** The TTP *pre*-IVCF placement in iFlow image. **(B)** The TTP *post*-IVCF placement in iFlow image.

**Abbreviations:** IVCF, inferior vena cava filter; TTP, time-to-peak.

The correlations between TNF- $\alpha$  content and RSF were performed using the models, revealing a positive association between TNF- $\alpha$  content and RSF levels.

## Discussion

This study established a porcine model to investigate NIH in the IVC induced by spindle-shaped IVCFs, with a particular emphasis on the association between caval wall neointimal thickness and RSFs driven from different ORs. It highlights the biomechanical response of the caval wall to varying mechanical stimuli generated by IVCFs with different ORs. In vitro study demonstrated that this non-physiological mechanical force—RSF—increased with the larger ORs of IVCF and IVC diameter. Further in vivo studies in swine were conducted to explore the potential relationship between RSFs and NIH thickness. The findings indicated that increased RSFs correlate non-linearly with greater NIH proliferation. Following the IVCF struts were immersed in the caval wall, vessel wall injury triggered a higher-level presence of TNF- $\alpha$ , which may be associated with the



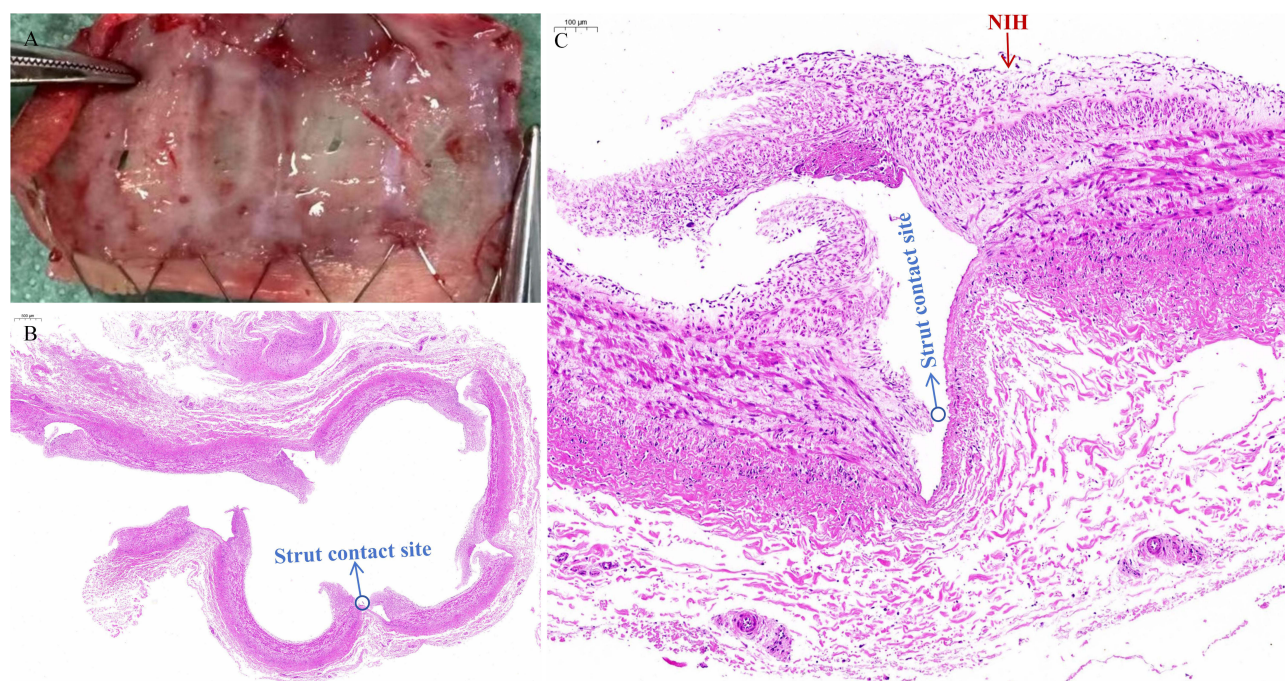


**Figure 4** Macroscopic and H&E characterization of IVC following IVCF placement. **(A)** Macroscopic examination revealed NIH at the site of IVCF placement, with more pronounced thickening in regions directly contacting the filter struts. **(B)** Histological analysis showed subintimal tissue overgrowth encapsulated the IVCF struts. **(C)** A magnified view of panel B, demonstrating disruption of the normal three-layered vessel wall, with marked thickening of the intima and thinning of the media and adventitia. **Abbreviations:** H&E, Hematoxylin & Eosin; IVC, inferior vena cava; IVCF, inferior vena cava filter; NIH, Neointimal hyperplasia.

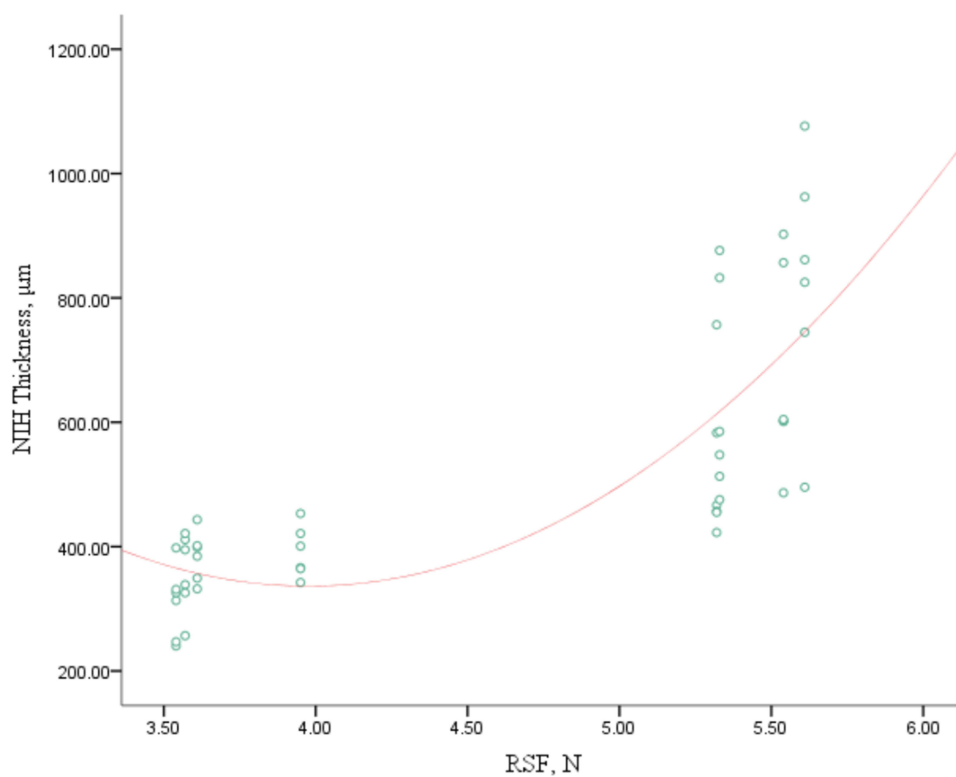


**Figure 5** NIH thickness increased with the enlarged RSFs, and regression analyses demonstrated a U-shaped relationship ( $R^2 = 0.630$ ,  $p < 0.001$ ), suggesting that NIH thickness consistently increase as the RSFs increase.

**Abbreviations:** NIH, neointimal hyperplasia; OR, oversizing ratio.



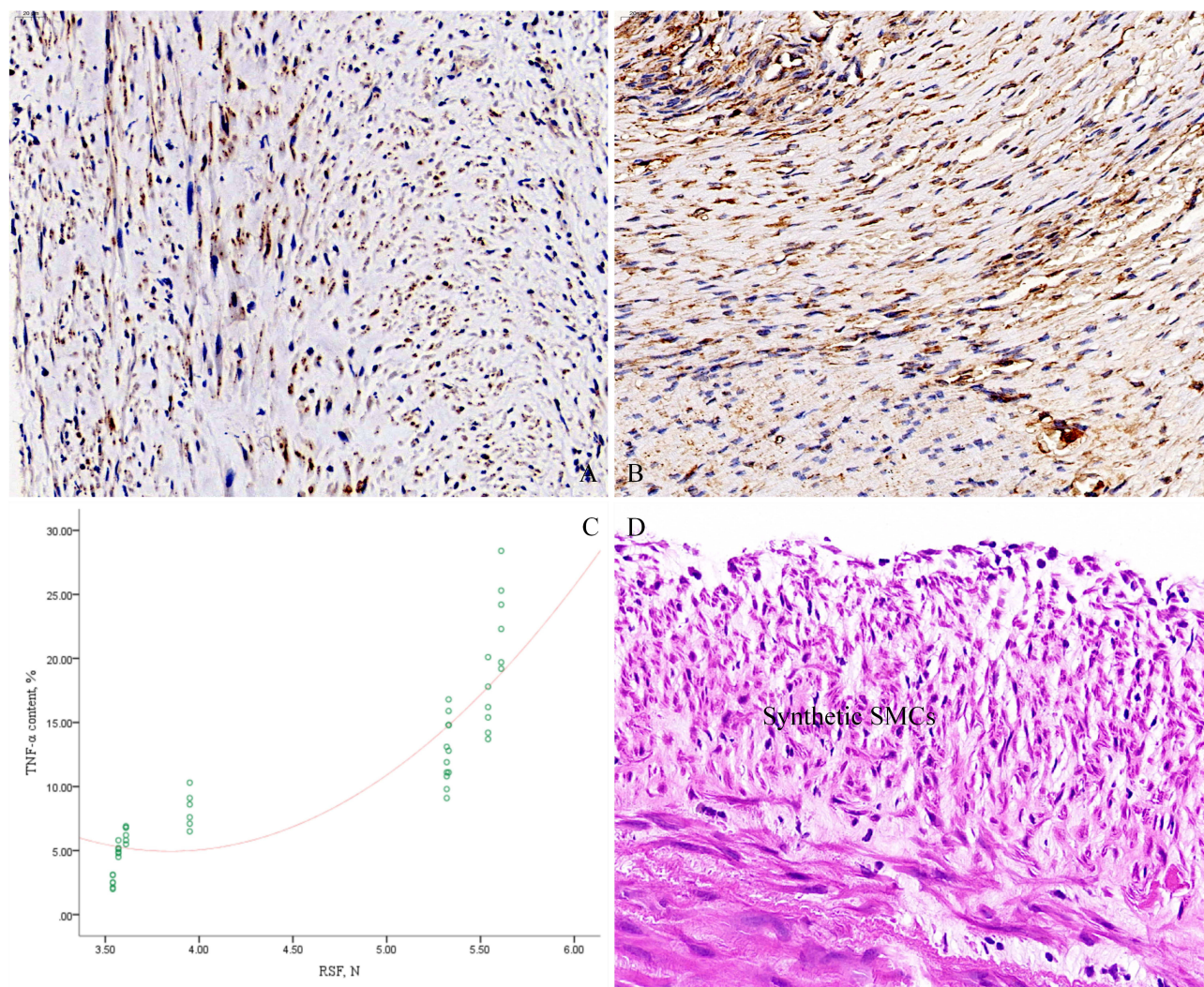


**Figure 6** Image analysis revealed the semiquantitative results of TNF- $\alpha$  deposition content in the porcine model following filter placement, as well as SMCs migration and proliferation in the 3rd week on hematoxylin and eosin. **(A)** An IVCF subjected to an RSF of 3.57 N exhibited a TNF- $\alpha$  content percentage of 5.8%. **(B)** An IVCF subjected to an RSF of 5.54 N had a TNF- $\alpha$  content percentage of 16.2%. **(C)** The relationship between TNF- $\alpha$  content percentage and RSF was confirmed by regression analyses, showing that an increased RSF positively correlates with increased NIH thickness. **(D)** Significant vessel response in the IVC wall after filter placement were observed, characterized by the proliferation of the vessel wall. RSF promotes the migration and proliferation of synthetic type SMCs (a flattened fibroblast-like state with a significantly increased cell volume compared to the contracted phenotype of VSMCs), thereby accelerating the NIH process.

**Abbreviations:** IVCF, inferior vena cava filter; NIH, neointimal hyperplasia; TNF- $\alpha$ , tumor necrosis factor-alpha; RSF, radial support force; SMCs, smooth muscle cells.

expression of matrix metalloproteinase (MMP) and promoting the migration and proliferation of SMCs, thereby accelerating the NIH process. Moreover, a positive correlation was identified between the increased RSFs and the TNF- $\alpha$  content.

The past few decades have witnessed animated discussions on the benefits of permanent IVCFs, partly due to the possible higher recurrence of DVT after eight years and no difference in long-term mortality.<sup>11</sup> The complications of IVCFs increase with dwell time, while the risk of PE often decreases over time. Retrievable IVCFs remain the mainstream option and are designed to be removed within a limited period or left permanently in place while necessary. Although the technique success rate of IVCF retrieval is high (80–93.4%),<sup>12</sup> difficulty or sometimes impossibility of retrieval is still an issue of IVCF retrieval. Histologic evidence of the IVC wall 124–1495 days following IVCF placement revealed scant native intima surrounded by a predominance of NIH and dense fibrosis.<sup>13</sup> By post-placement 20 days,<sup>14</sup> there was evidence of fibrosis with thick intimal proliferation and total filter strut involvement, contributing to retrieval difficulty. This is why we chose the 3rd week as the cut-off point. The major causes of retrieval failure for IVCFs were the inability to sheath the IVCF due to intimal overgrowth and the failure to engage the retrieval hook due to a severely tilted filter with an apex embedded into the caval wall.<sup>13</sup>

To date, no studies have detailed how the RSF exerted by IVCF affects NIH and surrounding tissues, although differences in RSF among IVCF models appear linked to vessel perforation rates.<sup>14</sup> While our previous study explored the relationship between OR and NIH,<sup>5</sup> the present study further investigates the deeper mechanisms that may lead to NIH from the perspective of RSF. In this study, the IVCF was selected based on its availability and real-world use at our institution. The data suggest that NIH may be the result of increased RSFs exerted by the mismatches in diameter between IVCF and IVC. More specifically, the increased RSFs correlate nonlinearly with greater NIH proliferation. This trend in caval NIH thickness parallels the RSF under constant conditions within a laboratory. Perhaps it is this increased RSFs applied to a relatively steady caval wall that predisposes the IVCF to NIH, higher forces exerted by this IVCF over a small IVC wall in an oversized manner may suggest a plausible mechanism for NIH. Thus, reducing RSFs may inhibit caval NIH, weaken the adhesion between the vascular wall and filter struts, increase retrieval success rates, and reduce vascular injury during retrieval. However, reduced RSFs may theoretically increase IVCF migration potential. Other factors may influence caval NIH, the dynamic changes in the IVC due to inspiration and expiration create a unique, fluctuating environment to which filters must adapt.<sup>15</sup> Hemodynamics analysis conducted before and after IVCF placement revealed no significant differences.

IVCF used has an anchor domain, which has the innate disadvantage of inadvertently causing damage to the IVC wall, which is not uncommon. Its notable consequence often observed is NIH. As reported, MMPs play a key role in extracellular matrix degradation, essential for cell migration into the intima following vessel injury. They are closely related to the proliferation, migration, and phenotype switch of SMCs.<sup>12,15–17</sup> Thors et al<sup>7</sup> reported a significant inflammatory response in IVC specimens 6 weeks after IVCF placement. Additionally, Zhang et al<sup>18</sup> found that TNF- $\alpha$  can induce the expression of MMPs. Research on the pathological role of TNF- $\alpha$  has been an active subject for more than half a century, yet the mechanisms regulated by TNF- $\alpha$  continue to intrigue researchers. TNF- $\alpha$  has been reported to exacerbate both atherosclerosis and restenosis, with several studies identifying its proinflammatory role in cardiovascular disease conditions and denotes an ongoing inflammation in different disease conditions. However, the study underlying NIH of the IVC following IVCF placement has not been well elucidated. Hence, we further investigated the role of TNF- $\alpha$  in NIH in the present study. As an acute phase reactant, the levels of TNF- $\alpha$  in animal studies were seen elevated within hours of stimulation with endotoxins, as noticed in acute lung, kidney, or liver injury. In this study, we found that TNF- $\alpha$  also participated in the caval NIH following IVCF placement and had a higher level. A positive correlation was also noted between the increased RSFs and the TNF- $\alpha$  content, which was attributable to increased RSFs potentially increasing intimal injury, inducing the expression of MMPs and promoting the migration and proliferation of SMCs, accelerating the NIH process.

Wang et al<sup>19</sup> revealed that human umbilical artery SMCs exhibited increases in the inflammatory factors, including IL-8, IL-6, IL-1 $\beta$ , vascular cell adhesion molecule-I, and intercellular adhesion molecule-I when subjected to high tensile force (> 10%) for 24 hours. Chou et al<sup>20</sup> reported that vascular endothelial injury can recruit inflammatory cells and amplify vascular inflammatory responses through the release of pro-inflammatory cytokines, notably TNF- $\alpha$ . This cascade promotes SMCs proliferation and enhanced migration, ultimately leading to phenotypic transformation. This in vitro study demonstrated that TNF- $\alpha$  enhanced the migratory ability of SMCs, a phenotypic change that can be inhibited by suppressing the Akt/AP-1 signaling pathway, thereby blocking TNF- $\alpha$ -induced cell migration. TNF- $\alpha$  can promote phenotypic transition of SMCs through upregulation of the RhoA/cyclin pathway. However, miR-145 can inhibit RhoA expression, thereby suppressing TNF- $\alpha$ -induced phenotypic transition of SMCs. In the present study, the increased TNF- $\alpha$  was also noted, suggesting that this inflammatory factor may participate in the phenotypic changes of SMCs after IVCF placement. As SMCs transition from a contractile state to a synthetic state, they participate in regulating the progression of NIH. Synthetic SMCs can generate a large amount of extracellular matrix and cytokines. Concurrently, their proliferative capacity is enhanced, triggering abnormal thickening of the vessel wall and luminal narrowing.<sup>9</sup>

This study has several limitations. Firstly, this model is restricted to a spindle-shaped filter design, which engages a larger surface area of the caval wall and thereby it may induce a more extensive degree of NIH.<sup>8</sup> Our selection of filters was restricted to this particular model as this was available at our institution and could be produced to different diameters. Other filter types, such as umbrella-shaped designs, were not included. Secondly, the study lacks of quantitative characterization of the stress-strain levels that precipitate cause caval injury. The mechanical stress exerted by the filter struts, which initiates vascular injury and subsequent neointimal formation, was not directly measured. Thirdly, the sample size for each filter diameter group was relatively small, which may limit the generalizability of the findings. Nonetheless, despite these constraints and the absence of



clinical validation, this model represents a meaningful step toward elucidating how RSFs from various ORs influence NIH progression. These insights may ultimately lead to the development of an IVCF that provides adequate caval interruption without the complications associated with NIH. Future investigations should also consider evaluating the performance of next-generation IVCF designs, particularly biodegradable filters. Unlike permanent or retrievable filters, biodegradable IVCFs have the potential to reduce or even eliminate long-term mechanical irritation following complete resorption, thereby possibly mitigating or resolving the NIH response. Preliminary studies have demonstrated promising biocompatibility and degradation characteristics of these materials in vascular setting.<sup>21,22</sup> Animal studies evaluating neointimal responses during and after filter resorption will be critical to determine their clinical applicability.

## Conclusions

Mechanical properties of IVCF such as RSF probably contribute, at least in part, to documented rates of NIH proliferation as a complication of filter placement. RSFs enlarged with the increased ORs of IVCF and IVC diameter. Evaluation of IVCF yielded a significantly higher RSF at a smaller caval diameter, with a higher-level presence of TNF- $\alpha$  during expansion, supporting a positive association with the greater NIH.

## Abbreviations

IVC, inferior vena cava; IVCF, inferior vena cava filter; TNF- $\alpha$ , tumor necrosis factor-alpha; NIH, neointimal hyperplasia; RSF, radial support force; OR, oversizing ratio; CVD, cardiovascular disease; DVT, deep vein thrombosis; PE, pulmonary embolism; SMC, smooth muscle cell; DSA, digital subtraction angiography; 3D, three-dimensional; ccDSA, color-coded digital subtraction angiography; ROIs, regions of interest; TTP, time-to-peak; SD, mean  $\pm$  standard deviation; CCC, concordance correlation coefficient; MMP, matrix metalloproteinase.

## Data Sharing Statement

The datasets generated and analyzed during the current study are not publicly available, as the study data are related to other studies that are progressing but are available from the corresponding author upon reasonable request.

## Ethical Approval and Consent to Participate

The study protocol was reviewed and approved by the institutional review board (IRB) of Nanjing First Hospital (NO. DWSY-23153536).

## Acknowledgments

This draft has been uploaded to Research Square as a preprint: <https://www.researchsquare.com/article/rs-5103222/v1>.

## Author Contributions

All authors made a significant contribution to the work reported, whether that is in the conception, study design, execution, acquisition of data, analysis and interpretation, or in all these areas; took part in drafting, revising or critically reviewing the article; gave final approval of the version to be published; have agreed on the journal to which the article has been submitted; and agree to be accountable for all aspects of the work.

## Funding

This work was supported by the Jiangsu Medical Association Special Fund Project [SYH-3201140-0088(2023035)], Nanjing Medical Science and Technology Development Project (YKK23116), and Nanjing Medical University Science and Technology Development Fund Project (NMUB20230163).

## Disclosure

The authors of this manuscript declare no relationships with any companies, whose products or services may be related to the subject matter of the article. The content of the manuscript is original, and it has not been published or accepted for publication.

## References

1. Wu H, Yang L, Luo R, et al. A drug-free cardiovascular stent functionalized with tailored collagen supports in-situ healing of vascular tissues. *Nat Commun.* 2024;15(1):735. doi:10.1038/s41467-024-44902-2
2. Boosani CS, Burela L. The exacerbating effects of the tumor necrosis factor in cardiovascular stenosis: intimal hyperplasia. *Cancers.* 2024;16(7):1435. doi:10.3390/cancers16071435
3. Barco S, Mahmoudpour SH, Planquette B, Sanchez O, Konstantinides SV, Meyer G. Prognostic value of right ventricular dysfunction or elevated cardiac biomarkers in patients with low-risk pulmonary embolism: a systematic review and meta-analysis. *Eur Heart J.* 2019;40(11):902–910. doi:10.1093/eurheartj/ehy873
4. Zhou D, Spain J, Moon E, McLennan G, Sands MJ, Wang W. Retrospective review of 120 Celect inferior vena cava filter retrievals: experience at a single institution. *J Vasc Interv Radiol.* 2012;23:1557–1563. doi:10.1016/j.jvir.2012.08.016
5. Gong M, Jiang R, He X, Gu J. Unveiling the link between oversizing ratio and neointimal hyperplasia in a porcine model. *Sci Rep.* 2025;15(1):10323. doi:10.1038/s41598-025-88585-1
6. Kuo WT, Cupp JS, Louie JD, et al. Complex retrieval of embedded IVC filters: alternative techniques and histologic tissue analysis. *Cardiovasc Interv Radiol.* 2012;35(3):588–597. doi:10.1007/s00270-011-0175-1
7. Thors A, Muck P. Resorbable inferior vena cava filters: trial in an in-vivo porcine model. *J Vasc Interv Radiol.* 2011;22(3):330–335. doi:10.1016/j.jvir.2010.11.030
8. Dowell JD, Castle JC, Schickel M, et al. Celect inferior vena cava wall strut perforation begets additional strut perforation. *J Vasc Interv Radiol.* 2015;26(10):1510–1518. doi:10.1016/j.jvir.2015.06.020
9. Jensen LF, Bentzon JF, Albarrán-Juárez J. The phenotypic responses of vascular smooth muscle cells exposed to mechanical cues. *Cells.* 2021;10(9):2209. doi:10.3390/cells10092209
10. Lou WS, Su HB, Huang KY, et al. Evaluation of distal hemodynamic changes of lower extremity after endovascular treatment: correlation between measurements of color-coded quantitative digital subtraction angiography and ankle-brachial index. *J Vasc Interv Radiol.* 2016;27(6):852–858. doi:10.1016/j.jvir.2016.02.011
11. PREPIC Study Group. Eight-year follow-up of patients with permanent vena cava filters in the prevention of pulmonary embolism: the PREPIC (Prevention du Risque d'Embolie Pulmonaire par Interruption Cave) randomized study. *Circulation.* 2005;112(3):416–422. doi:10.1161/CIRCULATIONAHA.104.512834
12. Xiao L, Wang M. MMP1 drug-eluting IVC filter decreases adhesion between caval wall and filter. *Cell Biochem Biophys.* 2013;65(2):159–161. doi:10.1007/s12013-012-9411-9
13. de Gregorio MA, Gimeno MJ, Tobio R, et al. Animal experience in the Günther Tulip retrievable inferior vena cava filter. *Cardiovasc Interv Radiol.* 2001;24(6):413–417. doi:10.1007/s00270-001-0063-1
14. Robins JE, Ragai I, Yamaguchi DJ. Differences in radial expansion force among inferior vena cava filter models support documented perforation rates. *J Vasc Surg Venous Lymphat Disord.* 2018;6(3):368–371. doi:10.1016/j.jvsv.2017.10.019
15. Sella DM, Oldenburg WA. Complications of inferior vena cava filters. *Semin Vasc Surg.* 2013;26:23–28. doi:10.1053/j.semvascsurg.2013.04.005
16. De Weese MS, Hunter DC Jr. A vena cava filter for the prevention of pulmonary emboli. *Bull Soc Int Chir.* 1958;17(1):17–25.
17. Kaufman JA, Barnes GD, Chaer RA, et al. Society of interventional radiology clinical practice guideline for inferior vena cava filters in the treatment of patients with venous thromboembolic disease: developed in collaboration with the American College of Cardiology, American College of Chest Physicians, American College of Surgeons Committee on Trauma, American Heart Association, society for vascular surgery, and society for vascular medicine. *J Vasc Interv Radiol.* 2020;31:1529–1544. doi:10.1016/j.jvir.2020.06.014
18. Zhang Y, Dong J, He P, et al. Genistein inhibit cytokines or growth factor-induced proliferation and transformation phenotype in fibroblast-like synoviocytes of rheumatoid arthritis. *Inflammation.* 2012;35(1):377–387. doi:10.1007/s10753-011-9365-x
19. Wang Z, Ashley DW, Kong L, Kang J, Nakayama DK, Dale PS. Nuclear factor-κB is activated in filter-implanted vena cava. *Cardiovasc Interv Radiol.* 2019;42(4):601–607. doi:10.1007/s00270-018-2138-2
20. Chou CC, Wang CP, Chen JH, Lin HH. Anti-atherosclerotic effect of hibiscus leaf polyphenols against tumor necrosis factor-α-induced abnormal vascular smooth muscle cell migration and proliferation. *Antioxidants.* 2019;8(12):620. doi:10.3390/antiox8120620
21. San Valentin EMD, Barcena AJR, Klusman C, Martin B, Melancon MP. Nano-embedded medical devices and delivery systems in interventional radiology. *Wiley Interdiscip Rev Nanomed Nanobiotechnol.* 2023;15(1):e1841. doi:10.1002/wnan.1841
22. Melancon ST, San Valentin EM, Bolinas DKM, et al. Fabrication of radiopaque, drug-loaded resorbable polymer for medical device development. *Polymers.* 2025;17(6):716. doi:10.3390/polym17060716

Journal of Inflammation Research

Publish your work in this journal

The Journal of Inflammation Research is an international, peer-reviewed open-access journal that welcomes laboratory and clinical findings on the molecular basis, cell biology and pharmacology of inflammation including original research, reviews, symposium reports, hypothesis formation and commentaries on: acute/chronic inflammation; mediators of inflammation; cellular processes; molecular mechanisms; pharmacology and novel anti-inflammatory drugs; clinical conditions involving inflammation. The manuscript management system is completely online and includes a very quick and fair peer-review system. Visit <http://www.dovepress.com/testimonials.php> to read real quotes from published authors.

Submit your manuscript here: <https://www.dovepress.com/journal-of-inflammation-research-journal>

**Dovepress**  
Taylor & Francis Group